Available online at www.sciencedirect.com
SCIENCE DIRECT
ELSEVIER
Journal of the European Ceramic Society 26 (2006) 2419–2425
ECERS
www.elsevier.com/locate/jeurceramsoc

Elastic characterization of CVD diamond by static and dynamic measurements

Luigi Bruno *, Leonardo Pagnotta, Andrea Poggialini

Dipartimento di Meccanica, Università della Calabria, Via Bucci CUBO44C, 87036 Arcavacata di Rende, Cosenza, Italy

Received 1 March 2004; received in revised form 27 March 2005; accepted 9 April 2005
Available online 17 May 2005

Abstract

The present paper describes two different nondestructive approaches for the direct identification of the elastic constants of thin square isotropic plates. First a static method is presented, by which the identification of the Young's modulus and Poisson's ratio is carried out by the full field measurement of the out-of-plane displacements detected on the upper surface of the plate in two biaxial bending tests. Then a dynamic method is illustrated, by which the elastic constants are determined from two different natural frequency of a free vibrating plate. Both techniques, previously verified on a carbon steel specimen, have been applied to a CVD diamond specimen; a comparison between the two approach is reported and the influence of the measurement errors is also discussed.

Keywords: Films; Non-destructive evaluation; Mechanical properties; CVD diamond; Diamond

1. Introduction

Nowadays the measurement of the elastic constants of the CVD diamond is typically carried out by a nanoindentation test.[1–3] This kind of technique is based on the determination of the load-displacement curve when some particular indenters (like the Berkovic or the corner-cube indenters) are used. The results obtained by this approach are highly dispersed because the dimensions of the indenters are of the same order of magnitude of the grain sizes. The use of these techniques is necessary when the CVD diamond is the coating of a substrate of different material. Other techniques that give highly dispersed results, like the laser ultrasonics, are available in literature.[4,5]

The elastic characterization of the CVD diamond is also troublesome when conventional tension or compression tests[6,7] are applied. The production of proper bulk specimens is not feasible owing to both the high cost of the material and its very brittle nature. Since the material can be plate shaped, the elastic characterization can be easily performed by bending or vibrating tests applied to a free-standing specimen. By this kind of specimen and by static or dynamic mechanical tests it is possible to obtain more repeatable results as shown in references[8–12]; on the other hand the mechanical tests imply loading set-up and alignment procedures usually complex, and the Poisson's ratio can not be measured accurately.

In the present paper both static and dynamic approaches have been applied to a CVD free-standing specimen. In the static approach two particular stress states are imposed on the specimen while the corresponding strain states are measured by speckle interferometry[13]; the elastic constants are evaluated by integral relations that do not require a numerical calibration. In the dynamic approach, the first and the third natural frequency of the free specimen are evaluated by applying an impulse excitation; the elastic constants are calculated from such frequencies by using polynomial functions obtained by an accurate numerical calibration.[14]

The specimen is a polycrystalline free-standing 50 mm × 50 mm plate with a uniform thickness of 0.4 mm. The deposition of the diamond was carried out at a temperature of 800–1000 °C and at a pressure of 10–100 mbar. The density, evaluated by measuring the volume (by the aforementioned

* Corresponding author. Tel.: +39 0984 49 4839; fax: +39 0984 49 4673.
E-mail addresses: bruno@unical.it (L. Bruno), pagnotta@unical.it (L. Pagnotta), poggialini@unical.it (A. Poggialini).

0955-2219/$ – see front matter © 2005 Elsevier Ltd. All rights reserved.
doi:10.1016/j.jeurceramsoc.2005.04.008

dimensions) and the mass (by a digital balance with a resolution of 0.001 g), is 3.412 g/cm^3. The porosity suggested by the owner of the specimen is about 4%.

2. The static approach

Theoretically the static approaches for the elastic characterization of a material require the measurement of the stress and strain state in a point. While it is easy to measure accurately the strains in a point (e.g. strain-gage), this is not true for the stresses, which in general are difficult to measure locally by an experimental technique. For this reason the stresses are evaluated, in the standard approaches, by adopting simple loading configurations, such as pure tension or pure bending,[6,15] which guarantee a uniform distribution of the stress components over a wide area.

An alternative way consists in adopting an integral approach[16–18]: in this case the stress components are evaluated by averaging the punctual quantities over a sufficiently wide area of the specimen (at worst the whole specimen). By this approach in some loading configurations it is possible to obtain an analytical expression of the average stress components, which is suitable for heterogeneous materials, such as composite materials, or for those materials whose mechanical behavior is influenced by the grain size; on the other hand the determination of the average strain components involves the use of more complex experimental techniques than the standard techniques based on strain-gages.

2.1. Theory

Fig. 1 shows the loading configuration adopted in the experimental tests: the specimen is supported on the three points P_i and loaded by a concentrated force at Q. By applying the principle of the virtual works the average stress components

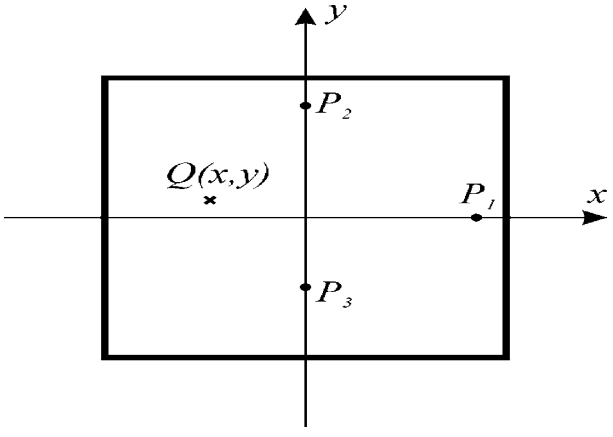

Fig. 1. The loading configuration: the specimen is supported on the three points P_i and loaded by a concentrated force applied at $Q(x, y)$.

$\bar{\sigma}_x, \bar{\sigma}_y, \bar{\tau}_{xy}$ can be evaluated by the following relations[16]:

$$\begin{Bmatrix} \bar{p}_\sigma \\ \bar{q}_\sigma \\ \bar{r}_\sigma \end{Bmatrix} = \begin{Bmatrix} \dfrac{\bar{\sigma}_x + \bar{\sigma}_y}{2} \\ \dfrac{\bar{\sigma}_x - \bar{\sigma}_y}{2} \\ \bar{\tau}_{xy} \end{Bmatrix} = \frac{3F}{Sh^2} \begin{Bmatrix} \dfrac{x(y_2y_3 + x_1^2 - xx_1) - x_1(y - y_2)(y - y_3)}{2x_1} \\ -\dfrac{x(y_2y_3 - x_1^2 + xx_1) - x_1(y - y_2)(y - y_3)}{2x_1} \\ -xy \end{Bmatrix}, \tag{1}$$

where F is the applied load, S and h are the area and the thickness of the specimen, respectively (x_i, y_i) the coordinates of the ith support points and (x, y) the coordinates of the point of application of the load. The quantities $\bar{p}_\sigma, \bar{q}_\sigma$ and $\bar{r}_\sigma$ are alternative parameters for describing the stress state. Therefore, by simply measuring the applied load it is possible to evaluate all the average stress components.

The corresponding average strain states are measured by a speckle interferometer sensitive to the out-of-plane displacements. By the procedure described in detail by the authors in[18] an analytical expression of the displacements is obtained for each stress state; then, by applying the definition of strain for a thin plate,[19] the strain components are calculated as:

$$\begin{Bmatrix} \bar{\varepsilon}_x \\ \bar{\varepsilon}_y \\ \bar{\gamma}_{xy} \end{Bmatrix} = -\frac{h}{2S} \int_S \begin{Bmatrix} \dfrac{\partial^2 w}{\partial x^2} \\ \dfrac{\partial^2 w}{\partial y^2} \\ 2\dfrac{\partial^2 w}{\partial x \partial y} \end{Bmatrix} \mathrm{d}S$$

$$\begin{Bmatrix} \bar{p}_\varepsilon \\ \bar{q}_\varepsilon \\ \bar{r}_\varepsilon \end{Bmatrix} = \begin{Bmatrix} \dfrac{\bar{\varepsilon}_x + \bar{\varepsilon}_y}{2} \\ \dfrac{\bar{\varepsilon}_x - \bar{\varepsilon}_y}{2} \\ \dfrac{\bar{\gamma}_{xy}}{2} \end{Bmatrix}, \tag{2}$$

where w are the out-of-plane displacements and $\bar{p}_\varepsilon, \bar{q}_\varepsilon$ and $\bar{r}_\varepsilon$ are, as in the case of the stresses, alternative parameters for describing the strain state.

Finally the elastic constants are evaluated by combining the average stress and strain components in two different loading configurations:

$$E = \frac{2\bar{p}_{\sigma I}\bar{q}_{\sigma S}}{\bar{p}_{\sigma I}\bar{q}_{\varepsilon S} + \bar{p}_{\varepsilon I}\bar{q}_{\sigma S}}, \qquad \nu = \frac{\bar{p}_{\sigma I}\bar{q}_{\varepsilon S} - \bar{p}_{\varepsilon I}\bar{q}_{\sigma S}}{\bar{p}_{\sigma I}\bar{q}_{\varepsilon S} + \bar{p}_{\varepsilon I}\bar{q}_{\sigma S}}, \tag{3}$$

where the subscripts *I* and *S* refer to isotropic and shear stress states.

Obviously, the values calculated by the above equations are affected by the inaccuracy of the single measurement of each factor involved. A significant dispersion in the tests is caused by the uncertainty of the location and of the measurement of the applied load and by the errors due to the procedure used for determining the average strains. To analyse the effects of these errors a considerable number of experimental tests must be carried out.

2.2. Results

The scheme of the experimental set-up is shown in Fig. 2: it is a Michelson interferometer. Along one arm there is the specimen placed in the loading device (Fig. 3), along the other arm there is a reference surface. The interferogram formed by the two speckle wavefronts produced by the specimen and the reference surface is observed by a CCD camera; by the analysis of the acquired images, the out-of-plane displacements of the specimen are determined pixel by pixel.

The loading device is formed by two knives (one for each loading configuration), two sliding platforms for the alignment of the points of the application of the loads, and a support base on which the specimen is laid. The load is applied by laying one or two steel spheres along the knives and is measured with a resolution of 10^{-3} N by a beam transducer (connected to a strain-gage amplifier) which supports the base and the specimen. More details about the loading device can be found in [18] where the whole procedure was previously tested on a carbon steel specimen whose elastic properties found in literature are well known. For completeness and clarity the results obtained for the steel are reported in Table 1.

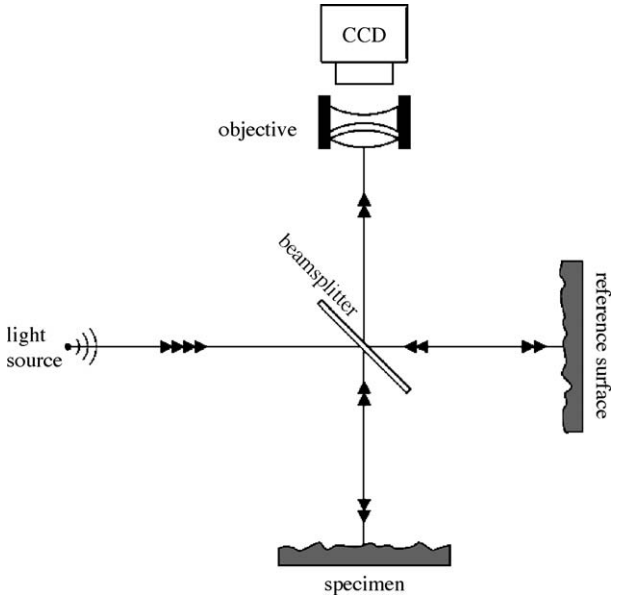

Fig. 2. Basic layout of the Michelson interferometer the measurement of the out-of-plane displacements.

On the CVD diamond specimen 51 tests was performed: 25 average isotropic stress states and 26 average shear stress states were randomly imposed on the specimen. By combining in all possible ways the results of the two sets of tests we have obtained 650 (=25 × 26) values for the Young's modulus and for the Poisson's ratio; these results are reported in Figs. 4 and 5. In these figures the dots represent the experimental results, the continuous lines indicate the mean value and the dashed lines represent the maximum deviations from the mean values. The mean values, the maximum deviations and the standard deviations of the elastic constants are re-

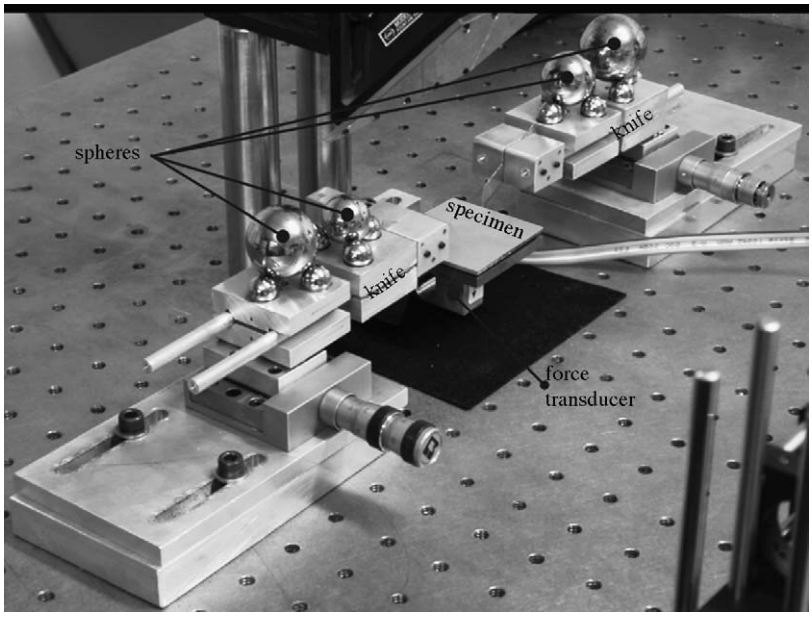

Fig. 3. The loading device: the specimen, placed on the force transducer, is loaded by steel spheres laid down on the two knives.

Table 1
Summary of the experimental results obtained for the steel specimen by the static approach

	Mean value	Standard deviation	Maximum deviation	Reference value
Young's modulus (GPa)	207.2	1.9	4.1	206
Poisson's ratio	0.297	0.011	0.023	0.290

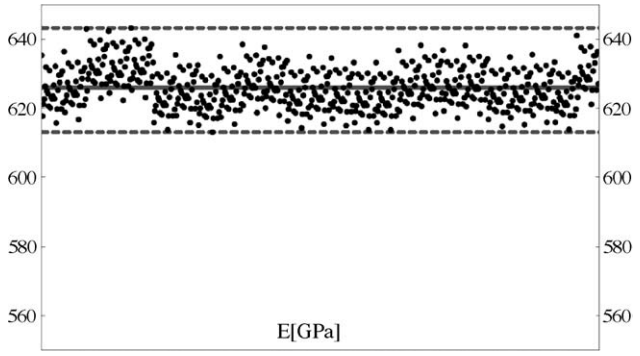

Fig. 4. The experimental set-up obtained for the Young's modulus.

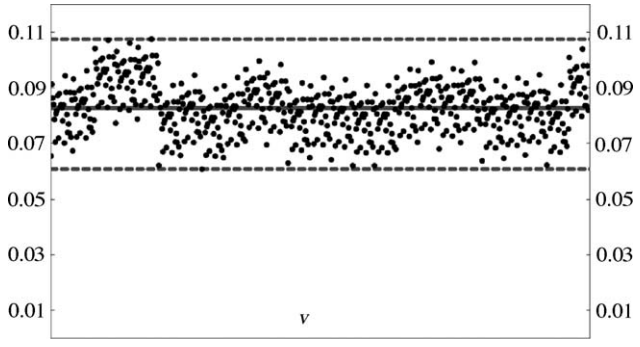

Fig. 5. The experimental set-up obtained for the Poisson's ratio.

ported in Table 2. It is interesting to note that the maximum deviations are approximately three times the standard deviations, as happens when the error distribution is gaussian. By taking into account the maximum error, the elastic constants measured by the static approach are:

$$\begin{matrix} E = 626 \pm 17\,\text{GPa} \\ \nu = 0.083 \pm 0.025 \end{matrix}. \quad (4)$$

Table 2
Summary of the experimental results obtained for the CVD diamond specimen by the static approach

	Mean value	Standard deviation	Maximum deviation
Young's modulus (GPa)	626.0	5.7	17.3
Poisson's ratio	0.083	0.009	0.025

3. The dynamic approach

The dynamic approaches are based on the relations between the mechanical resonance frequencies and the dynamic elastic constants of the material; this correlations depends on the geometry and on the mass of the specimen. Standards[20,21] suggest using bar-, rod- or circular plate-shaped specimens: they require the measurement of the natural frequency in two different modes of vibration and provide the procedures for determining the elastic constants. Flat plates of non circular shape can also be used, but the equations for determining the elastic constants are not provided by the standards and so must be evaluated separately.

In the present paper the elastic constants are determined from the first and the third natural frequency of a square plate of uniform thickness. For this purpose some suitable polynomial functions, obtained by an accurate numerical calibration, are employed. The natural frequencies are measured with a computerized measurement system using the impulse excitation technique. This procedure is described in detail in the following section.

3.1. Theory

The frequency equations of a thin isotropic linear-elastic square plate with free-free boundary conditions can be expressed in the following form[22,23]:

$$f_i = K_i(\nu)\sqrt{\frac{Et^3}{ml^2(1-\nu^2)}}, \quad (5)$$

where f_i represents the resonance frequency of the ith mode of vibration, E and ν are the elastic constants, m is the mass of the material, l and t are the edge and the thickness of the specimen, respectively. In general, K_i is a non-dimensional coefficient depending on the Poisson's ratio and on the ratio l/t; in the case of a thin plate ($l/t > 100$) the l/t dependence can be neglected. The variation of these coefficients with ν cannot be obtained analytically (no theoretical solutions are known for the case of a rectangular plate with free-free boundary conditions), but it can be found numerically.

The results of a numerical calibration, carried out by the commercial code MSC-Nastran, are reported in Figs. 6 and 7. Fig. 6 shows the variation of the coefficients K_i with the Poisson's ratio, while in Fig. 7 the variations of ν with different ratios of resonance frequencies (f_i/f_j) are reported. All curves given in Figs. 6 and 7 are plotted by joining the points obtained numerically by varying ν between 0.01 and 0.5 at steps of 0.01. A polynomial fitting of third degree describes the variation of each coefficient K_i with sufficient accuracy, two of these functions are reported in Table 3. A polynomial fitting of fourth degree is suitable to describe $\nu(f_i/f_j)$ (in the following $f_{ij} = f_i/f_j$); among the f_{ij}, f_{31} is the least sensitive function to the measurement errors on the ratio f_i/f_j, in fact, as can be seen in Fig. 7, the slope of this curve is the smallest. The expression of this function is reported in the last row of

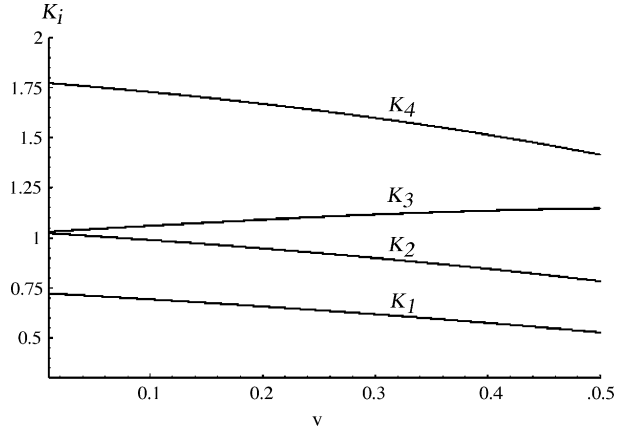

Fig. 6. Variation of the coefficient K_i with ν: the ith curve represents the variation with ν of the ith resonance frequencies normalized by the reference frequencies $\sqrt{Et^3/(ml^2(1-\nu^2))}$.

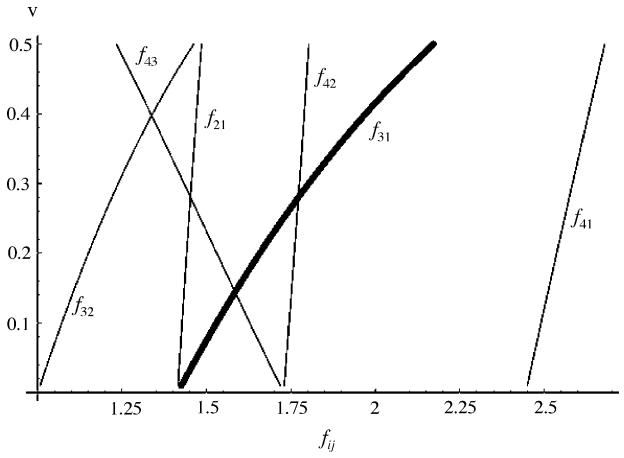

Fig. 7. Relation between Poisson's ratio and the ratios f_{ij}. By the measurement of f_{ij} it is possible to determine directly the Poisson's ratio. The slope of these curves is related to the sensitivity to the measurement error.

Table 3. By means of Table 3 and Eq. (5) it is possible to obtain E and ν according to the following steps:

1. measure the first and third resonance frequencies and calculate the ratio f_{31};
2. determine ν by the last equation of Table 3;
3. calculate one of the coefficients K_i by one of the first two equations of Table 3;
4. calculate E by Eq. (5).

3.2. Results

Fig. 8 shows the experimental equipment used for the measurement of the elastic constants. It is very simple and cheap, in fact it requires: a personal computer with sound input capabilities running in *LabVIEW* environment; a low cost directional microphone with a frequency response range of 10–20,000 Hz; some soft supports to cut the specimen off from external vibrations; an impulse tool.

Table 3
Analytical expression for the determination of the elastic constants by the measurement of the first and third resonance frequency

K_1	$0.7267 - 0.3191\nu - 0.1097\nu^2 - 0.09592\nu^3$
K_3	$1.028 + 0.3453\nu - 0.1374\nu^2 - 0.1585\nu^3$
ν	$-1.8702 + 1.5581 f_{31} + 0.085685 {f_{31}}^2 - 0.21996 {f_{31}}^3 + 0.040690 {f_{31}}^4$

Fig. 8. Experimental set-up for the measurement of the resonance frequencies.

The specimen is tapped lightly with the impulse tool causing a transient standing wave to be generated in the solid. The resulting sound is acquired by the microphone, recorded on the hard disk of the computer and analysed by a proper virtual instrument (VI). This extracts the frequency components of the sound by using a *fast fourier transform* algorithm; in addition, it also displays the waveform and frequency spectrum of the sound. A good resolution (less than 1 Hz) can be obtained. If the dimensions and mass of the solid are given, the elastic constants can then be calculated. The details about this experimental procedure are reported in ref.[14]; the results obtained by the dynamic technique for the same carbon steel specimen analysed by the static technique are reported in Table 4.

The uncertainty on E and ν can be evaluated by the well-known method for the analysis of uncertainty propagation using Taylor's series.[24] This approach can be adopted since an analytical expression relating the elastic constant to all the uncertainty quantities on which it depends is given (last equation in Table 3 and Eq. (5)). Dealing with absolute errors, the linear error propagation law can be used to carry out the error analysis of both the elastic constants.

According to the last equation of Table 3 the relative error on the Poisson's ratio depends on the ratio f_{31} and on the value of ν. The percentage error on the Poisson's ratio was evaluated by applying the theory of the uncertainty propagation: for very low values of ν, in order to obtain a percentage error less than 5%, it is necessary to measure the resonance

Table 4
Summary of the experimental results obtained for the steel specimen by the dynamic approach

	Mean value	Reference value
Young's modulus (GPa)	210.0	206
Poisson's ratio	0.290	0.290

Table 5
Measured resonance frequencies and the corresponding absolute and relative errors

	Measured value (Hz)	Absolute error (Hz)	Relative error (%)
f_1	1608	2	0.12
f_3	2412	2	0.08

Table 6
Summary of the experimental results obtained for the CVD diamond specimen by the dynamic approach

	Mean value	Maximum deviation
Young's modulus (GPa)	695	4
Poisson's ratio	0.075	0.003

frequencies with an error of about 0.04%; for typical values of ν (∼0.25), by an error of 0.2% on the frequencies, the error is less than 2%; finally for high values of ν (∼0.45) an error on the frequencies of 0.5% implies an error on the Poisson's ratio of about 2%. Therefore, in most of cases it is possible to obtain an error on ν less than 2%. As conservative hypothesis, a frequency measurement error of 2 Hz was assumed.

The error analysis on the Young's modulus is slightly more complex than the case of the Poisson's ratio, in fact, E is calculated as:

$$E = \frac{1-\nu^2}{K_i^2(\nu)} f_i^2 \frac{ml^2}{t^3}. \tag{6}$$

By applying the linear error propagation law the percentage error on the Young's modulus can be evaluated by the following formula:

$$\frac{\Delta E}{E} = \left| \frac{A_i \nu}{A_i \nu + B_i} \frac{\Delta \nu}{\nu} \right| + 2 \left| \frac{\Delta f_i}{f_i} \right|, \tag{7}$$

where the coefficients A_i and B_i are the parameters of the straight line by which it is possible to fit with a negligible error the first ratio in Eq. (6); of course these coefficients depend on the frequency used to evaluate E.

Table 5 reports the measured frequencies and the corresponding absolute and relative error; by these values and the values measured for the mass and dimensions of the specimen ($m = 3.412$ g, $l = 50$ mm, $t = 0.4$ mm) the elastic constants and the corresponding errors were evaluated:

$$\begin{aligned} E &= 695 \pm 4\,\text{GPa} \\ \nu &= 0.075 \pm 0.003 \end{aligned} \tag{8}$$

These results are reported in Table 6.

For the calculation of the Young's modulus both the first and the third frequency were used, but the values obtained were practically the same. Also for the uncertainty of E both frequencies were used. In this case slightly different results were obtained, in Eq. (6) the greater value is used.

4. Conclusions

In the present paper the elastic characterization of a CVD diamond specimen has been carried out by a static and a dynamic experimental technique. Apart from the Poisson's ratio measured by the static approach, both the techniques have provided highly repeatable results. In particular, relative errors of less than 3 and 1% for the static and dynamic Young's modulus, respectively, were obtained. A maximum error of about 4% was obtained for the dynamic Poisson's ratio while a high relative error (∼30%) was obtained in the static measurements.

The discrepancies between the dynamic and static results are due to many causes. In the dynamic measurements, the elastic constants are obtained from the dynamic behaviour of the specimen and therefore, such data reflect the frequency dependence of the material. Furthermore, the finite element model assumed in the numerical calibration provides only approximate results, both for the kind of the solution adopted and for neglecting the damping effects of the material. In the static measurements some systematic error sources affect the measurements, such as the identification of the coordinate system on the image of the specimen and the location of the support points. Finally, the different thermal conditions governing the tests (the static test is an isothermal test, whereas the dynamic test is essentially adiabatic) could generate further differences. Of course additional errors due to the measurement of the geometry of the specimen (the edge and the thickness) can also influence the measurements in both the techniques.

Finally we can state that the proposed techniques are easy and quick to perform, so by them it is possible to obtain a large amount of data in a short time; in addition, the dynamic technique requires a very cheap experimental set-up. The estimated values for the Young's modulus have shown a very small dispersion if compared with that obtained by the techniques based on the nanoindentation tests. For the Poisson's ratio very few results are available in literature and usually this parameter cannot be measured, instead by the proposed techniques it is possible to achieve a good accuracy and repeatability.

References

1. Pharr, G. R. and Oliver, W. C., An improved technique for determining hardness and elastic modulus using load and displacement sensing indentation experiments. *J. Mater. Res.*, 1992, **7**(6), 1564–1583.
2. Furgiuele, F. M., Sciumè, G., De Fazio, L., Syngellakis, S. and Wood, R. J. K., Nanoindentation of CVD diamond: comparison of FE model with analyitcal and experimental data. *Diamond Relat. Mater.*, 2001, **10**, 765–769.
3. Beghini, M. and Bertini, L., *Identificazione della curva tensione-deformazione di acciai sulla base di prove di durezza strumentate*. XXVIII Convegno Nazionale AIAS, Vicenza, 1999, pp. 597–606.
4. Qian, M. L., Hu, W. X., Xu, W. J., Jenot, F. and Ourak, M., Determination of surface elastic constants of CVD diamond sheet by laser

ultrasonics, *AIP Conference Proceedings*, April 30, 2001. Vol 557, Issue 1, 1383–1388.
5. Philip, J., Hess, P., Feygelson, T., Butler, J. E., Chattopadhyay, S., Chen, K. H. *et al.*, Elastic, mechanical, and thermal properties of nanocrystalline diamond films. *J. Appl. Phys.*, 2003, **93**(4), 2164–2171.
6. ASTM E111-97, Standard test method for young's modulus, tangent modulus, and chord modulus. *Annual Book Of ASTM Standard*, *Vol 03–01*.
7. ASTM D3148-02, Standard test method for elastic moduli of intact rock core specimen in uniaxial compression. *Annual Book Of ASTM Standard*, *Vol 04–08*.
8. Valentine, T. J., Whitehead, A. J., Sussmann, R. S., Wort, C. J. H. and Scarsbrook, G. A., Mechanical property measurements of bulk polycrystalline CVD diamond. *Diamond Relat. Mater.*, 1994, **3**, 1168–1172.
9. Werner, M., Klose, S., Szücs, F., Molle, C., Fecht, H. J., Johnston, C. *et al.*, High temperature Young's modulus of polycrystalline diamond. *Diamond Relat. Mater.*, 1997, **6**, 344–347.
10. Szuecs, F., Werner, M., Sussmann, R. S., Pickles, C. S. J. and Fecht, H. J., Temperature dependence of Young's modulus and degradation of chemical vapor deposited diamond. *J. Appl. Phys.*, 1999, **86**(11), 6010–6017.
11. D'Evelyn, M. P. and Taniguchi, T., Elastic properties of translucent polycrystalline cubic boron nitride as characterized by the dynamic resonance method. *Diamond Relat. Mater.*, 1999, **8**, 1522–1526.
12. Werner, M., Kohler, T., Mietke, S., Worner, E., Johnston, C. and Fecht, H. J., Review on the non-destructive characterization and application of doped and undoped polycrystalline diamond films. *Proc. SPIE*, 2002, **4703**, 199–210.
13. Erf, R. K., ed., *Speckle Metrology*. Academic Press, New York, 1978.
14. Alfano, M., Bruno, L. and Pagnotta, L., *Determinazione delle Costanti Elastiche di Piastre Quadrate Isotrope dalle Frequenze Naturali di Vibrazione*. XXXII Convegno Nazionale AIAS, Salerno, 2003.
15. ASTM D6272-02, Standard test method for flexural properties of unreinforced and reinforced plastics and electrical insulating materials by four-point bending. *Annual Book Of ASTM Standard*, *Vol 08–03*.
16. Grediac, M. and Vautrin, A., A new method for determination of bending rigidities of thin anisotropic plates. *J. Appl. Mech. Trans. ASME*, 1990, **57**, 964–968.
17. Bruno, L., Furgiuele, F. M., Pagnotta, L. and Poggialini, A., A full-field approach for the elastic characterization of anisotropic materials. *Opt. Lasers Eng.*, 2002, **37**(4), 417–431.
18. Bruno, L. and Felice, G., An innovative approach for the elastic characterization of anisotropic materials. In *Proc. Compos. Constructions*, 2003, pp. 177–182.
19. Gibson, R. F., *Principle of composite material mechanics*. McGraw Hill, Singapore, 1994.
20. ASTM E1875-01, Standard test method for dynamic young's modulus, shear modulus, and Poisson's ratio by sonic resonance. *Annual Book Of ASTM Standard*, *Vol 03–01*.
21. ASTM E1876-00e1, standard test method for dynamic young's modulus, shear modulus, and poisson's ratio by impulse excitation of vibration. *Annual Book Of ASTM Standard*, *Vol 03–01*.
22. Young, D., Vibration of rectangular plates by the Ritz method. *J. Appl. Mechanics (ASME)*, 1950, **17**, 448–453.
23. Shuyu, L., Study on the flexural vibration of rectangular thin plates with free boundary conditions. *J. Sound Vibration*, 2001, **239**(5), 1063–1071.
24. Sydenham, P. H., Hancock, N. H. and Thorn, R., *Introduction to Measurement Science and Engineering*. J. Wiley & Sons, UK, 1993.